Supporting Information: Benthic biolayer structure controls whole-stream reactive transport

Kevin R. Roche and Marco Dentz*

Department of Civil Engineering, Boise State University, Boise, ID and
Spanish National Research Council (IDAEA-CSIC), Barcelona, Spain
(Dated: October 31, 2021)

CONTENTS

SI-I.   FLOW AND MIXING PROFILES

We employ the following velocity profile

$$v(z) = \overline{v} + v_0/\kappa[1 + \ln(z/d)] \tag{S1}$$

where $\overline{v}$ is the average velocity over the full vertical cross section between the sediment-water interface (SWI) at $z = 0$ and the air-water interface at $z = d$. We introduce the length z_0, which represents a porous layer on the SWI, and we set $v(z) = 0$ for $z < z_0$. This implies that $v(z_0) > 0$ represents the slip velocity at the SWI. In this sense, we rewrite expression (S1) as follows

$$v(z) = v(z_0) + \overline{v} + v_0 \kappa^{-1} \left[1 + \ln[(z/d)] - (\overline{v} + v_0/\kappa[1 + \ln(z_0/d)]) \right] \tag{S2}$$

Setting $v(z_0) \equiv v_s$, we write

$$v(z) = v_s + v_0 \kappa^{-1} \ln[(z/z_0)]. \tag{S3}$$

Vertical mixing is represented by the dispersion coefficient [1]

$$D(z) = v_0^2 (1 - z/d) \frac{1}{\mathrm{d}v\,(z)/\mathrm{d}z} = v_0 z \kappa (1 - z/d) \tag{S4}$$

for $z > z_0$. At $z < z_0$, we set $D(z) = D_h$.

---

* E-mail: kevinroche@boisestate.edu

SI-II. MOBILE-IMMOBILE BIOLAYER (MIM-B) MODEL

A. Vertical Average

In order to upscale the reactive transport problem, we employ a dual porosity approach and separate the transport equation (1) in the main manuscript into an equation that describes advection-dispersion in the river,

$$\frac{\partial C_s}{\partial t} + v(z)\frac{\partial C_s}{\partial x} - \nabla \cdot [D(z)\nabla C_s] = 0, \tag{S5a}$$

and an equation for diffusion-reaction in the hyporheic zone

$$\theta_h \frac{\partial C_h}{\partial t} - D_h \theta_h \frac{\partial C_h}{\partial z^2} = -k(z)\theta_h C_h, \tag{S5b}$$

where the concentrations in the river and hyporheic zone (HZ) are denoted by C_s and C_h, respectively, θ_h is the porosity in the hyporheic zone (assumed constant), and $D(z)$ is the effective vertical diffusion coefficient. Note that diffusion in direction of the stream is disregarded here because it is considered very small compared to the effects of shear dispersion. Both domains are coupled through concentration and flux continuity at the interface located at $z = 0$,

$$C_h(x, z = 0, t) = C_s(x, 0, t) \tag{S6}$$

$$D(z) \left.\frac{\partial C_s}{\partial z}\right|_{z=0} = D_h \theta_h \partial_z C_h|_{z=0} \tag{S7}$$

We define now the vertical average over the stream as

$$\overline{C}_s = \frac{1}{d} \int_0^d \mathrm{d}z\, C_s. \tag{S8}$$

Vertical averaging of Eq. (S5) gives

$$\frac{\partial \overline{C}_s}{\partial t} + \overline{v}\frac{\partial \overline{C}_s}{\partial x} - D^* \frac{\partial^2 \overline{C}_s}{\partial x^2} = -\left.\theta_h D_h \frac{\partial C_h}{\partial z}\right|_{z=0}, \tag{S9}$$

where we use flux-continuity at the interface expressed by Eq. (S7), and D^* is the shear dispersion coefficient defined in the main text. The diffusive flux on the right side can be expressed in terms of the accumulation and reaction terms in the hyporheic zone by integrating Eq. (S5a) over z. This gives

$$\left.\theta_h D_h \frac{\partial C_h}{\partial z}\right|_{z=0} = \theta_h \frac{\partial}{\partial t} M_h + \int_{-h}^0 \mathrm{d}z\, k(z)\theta_h C_h, \tag{S10}$$

where we defined the vertically integrated concentration M_h in the hyporheic zone as

$$M_h = \int_{-h}^0 \mathrm{d}z\, C_h. \tag{S11}$$

Thus, we can write the following evolution equation for the average concentration $\overline{C}_s$ in the stream,

$$\frac{\partial}{\partial t}\left(\overline{C}_s + \frac{\theta_h}{d} M_h\right) + \overline{v}\frac{\partial \overline{C}_s}{\partial x} - D^* \frac{\partial^2 \overline{C}_s}{\partial x^2} = -\frac{1}{d}\int_{-h}^0 \mathrm{d}z\, k(z)\theta_h C_h, \tag{S12}$$

The term on the right side of (S12) represents a sink term for the stream domain due to reactions in the hyporheic zone. The derivation of the vertical average in the stream gives rise to the shear dispersion coefficient, which quantifies the impact of velocity variability with depth on longitudinal dispersion [1].

B. Closure

In order to close Eq. (S12), we need to express M_h and the right side in terms of $\overline{C}_s$. As a first step, we approximate the interface condition (S6) by

$$C_h(x, z = 0, t) = \overline{C}_s(x, t), \tag{S13}$$

which assumes that concentration in the stream is uniform in the vertical. Furthermore, invoking the Duhamel's theorem [2], we note that the solution of Eq. (S5b) can be written as

$$C_h = \int_0^t dt'\, g(z, t - t')\overline{C}_s(x, t'), \tag{S14}$$

where the Green function $g(z, t)$ satisfies

$$\frac{\partial g}{\partial t} - D_h \frac{\partial^2 g}{\partial z^2} = -k(z)g. \tag{S15}$$

for the boundary condition $g(z = 0, t) = \delta(t)$. Thus, we can write (S11) as

$$M_h = \int_0^t dt'\, \varphi_h(t - t')\overline{C}_s(x, t'), \tag{S16}$$

where the memory function

$$\varphi_h(t) = \int_{-h}^0 dz\, g(z, t), \tag{S17}$$

denotes the mass in the hyporheic zone in response to an instantaneous solute pulse at the SWI. The reaction term on the right side of Eq. (S12) is given by

$$\theta_h \int_{-h}^0 dz\, k(z)C_h = \theta_h \int_0^t dt'\, \varphi_r(t')\overline{C}_s(z, t - t'), \tag{S18}$$

where we defined the reactive memory function $\varphi_r(t)$ by

$$\varphi_r(t) = \int_{-h}^0 dz\, k(z)g(z, t). \tag{S19}$$

Thus, Eq. (S12) can be written as

$$\frac{\partial}{\partial t}\overline{C}_s + \frac{\theta_h}{d} \frac{\partial}{\partial t} \int_0^t dt'\, \varphi_h(t - t')\overline{C}_s(x, t') + \overline{v}\frac{\partial \overline{C}_s}{\partial x} - D^*\frac{\partial^2 \overline{C}_s}{\partial x^2} = -\frac{\theta_h}{d} \int_0^t dt'\, \varphi_r(t')\overline{C}_s(z, t - t'). \tag{S20}$$

Note that closed form expressions for the Green function $g(z, t)$ for arbitrary reaction profiles are generally not available. In the following, we solve this problem for the biolayer reaction scenario.

C. Biolayer

For the reaction profile $k(z) = k_b \mathbb{I}(-b < z < 0)$, the reactive memory function (S19) can be written as

$$\varphi_r(t) = k_b \varphi_b(t). \tag{S21}$$

where we defined

$$\varphi_b(t) = \int_{-b}^{0} \mathrm{d}z \, g(z,t). \tag{S22}$$

In order to determine explicit expresions for the memory function, we solve now Eq. (S15) for the Green function. For convenience, we define a local coordinate system such that the interface between the biolayer and the sublayer is located at $z' = 0$, the interface between stream and streambed is located at $z' = b$, and the lower boundary of the hyporheic zone is located at $z' = b - h \equiv -\ell$. In the following we omit the primes for compactness of notation. We separate Eq. (S15) for the hyporheic zone into two coupled equations, one for the biolayer and one for the sublayer. The equation for the Green function $g_b(z,t)$ in the biolayer is

$$\frac{\partial g_b}{\partial t} - D_h \frac{\partial^2 g_b}{\partial z^2} = -k_b g_b \tag{S23a}$$

for the initial condition $g_b(z, t = 0) = 0$ and the boundary condition $g_b(z = b, t) = \delta(t)$. The equation for the concentration $g_0(z,t)$ in the sublayer is

$$\frac{\partial g_0}{\partial t} - D_h \frac{\partial^2 g_0}{\partial z^2} = 0. \tag{S23b}$$

At the interface between biolayer and sublayer at $z = 0$, we have concentration and flux continuity, that is, $g_b = g_0$ and $\partial g_b/\partial z = \partial g_0/\partial z$. The boundary condition for g_0 at $z = -\ell$ is $\partial g_0/\partial z = 0$.

In order to solve for the Green functions g_b and g_0, we consider the system (S23) in Laplace space. Laplace transformed quantities in the following are marked by an asterisk, and the Laplace variable is denoted by λ (i.e., $g^* = \int_0^\infty \mathrm{d}t \, e^{-\lambda t} g$, [3]). Thus, we obtain for (S23a)

$$\lambda g_b^* - D_h \frac{\partial^2 g_b^*}{\partial z^2} = -k_b g_b^* \tag{S24a}$$

and the boundary condition $g_b^*(z = b, \lambda) = 1$. The Laplace transform of (S23b) is given by

$$\lambda g_0^* - D_h \frac{\partial^2 g_0^*}{\partial z^2} = 0. \tag{S24b}$$

At the interface at $z = 0$, we have

$$g_b^* = g_0^*, \qquad\qquad \frac{\partial g_b^*}{\partial z} = \frac{\partial g_0^*}{\partial z}. \tag{S25}$$

Thus, the Laplace transform of $g_0(z,t)$ in the sublayer can be expressed in terms of the concentration $g_b^*(z = 0, \lambda)$ as

$$g_0^*(z, \lambda) = G^*(z, \lambda) g_b^*(z = 0, \lambda), \tag{S26}$$

where the Green function $G^*(z, \lambda)$ satisfies (S24b) for the boundary condition $G = 1$ at $z = 0$. It is given by

$$G^*(z, \lambda) = \frac{\cosh(\sqrt{\lambda \tau_0}(1 + z/\ell))}{\cosh(\sqrt{\lambda \tau_0})}, \tag{S27}$$

where we defined $\tau_0 = \ell^2/D_h$.

The fundamental solution for $g_b^*(z, \lambda)$ is

$$g_b^*(z, \lambda) = A \exp(-zB) + C \exp(zB), \qquad\qquad B = \sqrt{(\lambda + k_b)/D_h}, \tag{S28}$$

where the constants A and C are determined from the Dirichlet boundary condition at $z = 0$ and the Neumann boundary condition at $z = b$. Note that concentration continuity at $z = 0$ is automatically fulfilled by (S26). Thus, we obtain the solution

$$g_b^*(z, \lambda) = \frac{\cosh(\sqrt{(\lambda + k_b)\tau_b} \, z/b) + \sqrt{\frac{\lambda}{\lambda + k_b}} \tanh(\sqrt{\lambda \tau_0}) \sinh(\sqrt{(\lambda + k_b)\tau_b} \, z/b)}{\cosh(\sqrt{(\lambda + k_b)\tau_b}) + \sqrt{\frac{\lambda}{\lambda + k_b}} \tanh(\sqrt{\lambda \tau_0}) \sinh(\sqrt{(\lambda + k_b)\tau_b})}. \tag{S29}$$

The total mass φ_b in the biolayer in response to an instantaneous unit pulse at the interface at $z = b$ is given by its Laplace transform as

$$\varphi_b^*(\lambda) = \int_0^b \mathrm{d}z\, g_b^*(z, \lambda) = \sqrt{\frac{D_h}{\lambda + k_b}} \frac{\sinh(\sqrt{(\lambda + k_b)\tau_b}) + \sqrt{\frac{\lambda}{\lambda + k_b}} \tanh(\sqrt{\lambda\tau_0}) \left[\cosh(\sqrt{(\lambda + k_b)\tau_b}) - 1\right]}{\cosh(\sqrt{(\lambda + k_b)\tau_b}) + \sqrt{\frac{\lambda}{\lambda + k_b}} \tanh(\sqrt{\lambda\tau_0}) \sinh(\sqrt{(\lambda + k_b)\tau_b})} \tag{S30}$$

Furthermore, we obtain for the concentration $g_0^*(z, \lambda)$ in the sublayer,

$$g_0^*(z, \lambda) = \frac{G^*(z, \lambda)}{\cosh(\sqrt{(\lambda + k_b)\tau_b}) + \sqrt{\frac{\lambda}{\lambda + k_b}} \tanh(\sqrt{\lambda\tau_0}) \sinh(\sqrt{(\lambda + k_b)\tau_b})} \tag{S31}$$

The mass φ_0 in the sublayer in terms of its Laplace transform is

$$\varphi_0^*(\lambda) = \int_{-\ell}^0 \mathrm{d}z\, g_0^*(z, \lambda) = \sqrt{\frac{D_h}{\lambda}} \frac{\tanh(\sqrt{\lambda\tau_0})}{\cosh(\sqrt{(\lambda + k_b)\tau_b}) + \sqrt{\frac{\lambda}{\lambda + k_b}} \tanh(\sqrt{\lambda\tau_0}) \sinh(\sqrt{(\lambda + k_b)\tau_b})} \tag{S32}$$

The Laplace transform $\varphi_h^*(\lambda)$ of the memory function φ_h, which denotes the mass in the hyporheic zone in response to Delta pulse at the stream-streambed interface, is thus given by

$$\varphi_h^*(\lambda) = \varphi_b^*(\lambda) + \varphi_0^*(\lambda). \tag{S33}$$

In conclusion, we can write the governing equation (S20) for $\overline{C}_s$ as

$$\frac{\partial}{\partial t}\overline{C}_s + \frac{\theta_h}{d}\frac{\partial}{\partial t}\int_0^t \mathrm{d}t'\, \varphi_h(t - t')\overline{C}_s(x, t') + \overline{v}\frac{\partial \overline{C}_s}{\partial x} - D^*\frac{\partial^2 \overline{C}_s}{\partial x^2} = -\frac{\theta_h k_b}{d}\int_0^t \mathrm{d}t'\, \varphi_b(t - t')\overline{C}_s(x, t'). \tag{S34}$$

Note that the vertically integrated concentration M_b in the biolayer is given in terms of the biolayer memory function $\varphi_b(t)$ as

$$M_b = \int_0^t \mathrm{d}t'\, \varphi_b(t - t')\overline{C}_s(x, t'). \tag{S35}$$

D. Mass balance

The mass conservation equation for the benthic biolayer is obtained by integrating Eq. (S23a) from 0 to b. This gives

$$\frac{\mathrm{d}\varphi_b}{\mathrm{d}t} = -D_h\frac{\partial g_b(z = 0)}{\partial z} + D_h\frac{\partial g_b(z = b)}{\partial z} - k_b\varphi_b. \tag{S36}$$

The first and second terms on the right hand side denote mass transfer across the interfaces with the sublayer and the stream, the third term is a sink term due to reaction. Using flux continuity over the interface at $z = 0$, we can express the right side in terms of the mass φ_0 in the sublayer as

$$\frac{\mathrm{d}\varphi_b}{\mathrm{d}t} = -\frac{\mathrm{d}\varphi_0}{\mathrm{d}t} + D_h\frac{\partial g_b(z = b)}{\partial z} - k_b\varphi_b, \tag{S37}$$

The reacted mass m_R is obtained from

$$\frac{\mathrm{d}m_R(t)}{\mathrm{d}t} = k_b\varphi_b(t) \tag{S38}$$

and therefore

$$m_R^\infty = k_b\varphi_b^*(\lambda = 0). \tag{S39}$$

From the explicit expression (S30), we obtain

$$m_R^\infty = \sqrt{\frac{D_h}{k_b}} \tanh(\sqrt{k_b \tau_b}). \tag{S40}$$

where $\tau_b = b^2/D_h$. For times $t \gg \tau_b$, that is, for times much larger than the time for complete mixing of the biolayer, we set g_b equal to the mean concentration in the biolayer,

$$g_b = \frac{\varphi_b}{b}. \tag{S41}$$

Furthermore, we approximate the derivative of g_b at $z = b$ as

$$\frac{\partial g_b}{\partial z} = -\frac{g_b}{b} = -\frac{\varphi_b}{b^2}. \tag{S42}$$

With this approximation, the mass balance equation (S37) can be written as

$$\frac{\mathrm{d}\varphi_b}{\mathrm{d}t} = -\frac{\mathrm{d}\varphi_0}{\mathrm{d}t} - \frac{D_h}{b^2}\varphi_b - k_b\varphi_b, \tag{S43}$$

We can furthermore write

$$\frac{\mathrm{d}\varphi_b}{\mathrm{d}t} = -\frac{\mathrm{d}\varphi_0}{\mathrm{d}t} - \frac{1 + Da}{\tau_b}\varphi_b. \tag{S44}$$

The solution of this equation can be obtained by separation of variables as

$$\varphi_b(t) = \frac{b}{\tau_b} \exp(-\alpha t) - \int_t^\infty \mathrm{d}t' \, \exp[-\alpha(t - t')]\frac{\mathrm{d}\varphi_0(t')}{\mathrm{d}t'}, \tag{S45}$$

where we defined $\alpha = (1 + Da)/\tau_b$, and used the initial condition $\varphi_b(t = 0) = b/\tau_b$. This initial condition is obtained from the solution of the equivalent conservative problem, that is, for $k_b = 0$ in (S43) and using mass conservation (the integral over all times equal to one), because at $t = 0$, the two solutions should coincide. Note that the approximation made here for calculation $\varphi_b(t)$ are valid at times $t > \tau_b$. We know that the early time behavior is otherwise different from the exact solution (S30).

For $\alpha t \gg 1$, the first terms on the right side of (S45) can be disregarded, and the integral can be localized at $t' = t$. That is, as the exponential is sharply peaked about $t = t'$, we can set

$$\varphi_b(t) = -\frac{\mathrm{d}\varphi_0(t)}{\mathrm{d}t} \int_t^\infty \mathrm{d}t' \, \exp[-\alpha(t - t')]. \tag{S46}$$

Thus, we obtain

$$\varphi_b(t) = -\frac{\tau_b}{1 + Da}\frac{\mathrm{d}\varphi_0(t)}{\mathrm{d}t}. \tag{S47}$$

This implies, the mass in the biolayer scales as the time derivative of the mass in the sublayer.

SI-III. ANALYTICAL LAPLACE SPACE SOLUTIONS

In the following we provide explicit analytical solutionz for the breakthrough curves in the MIM-B and the *S1* models.

A. Stream concentration in the MIM-B model

We solve Equation (S34) for the boundary condition $\overline{C}_s(x = 0, t) = \delta(t)$. To this end, we transform (S34) to Laplace space, which gives

$$\lambda \overline{C}_s^* + \theta_h d^{-1}[\lambda \varphi_h^*(\lambda) + k_b \varphi_b^*(\lambda)]\overline{C}_S^*(x, \lambda) + \overline{v}\partial_x \overline{C}_S^*(\lambda) - D^* \partial_x^2 \overline{C}_s^*(\lambda) = 0. \tag{S48}$$

The boundary condition reads as

$$\overline{C}_s(x = 0, \lambda) = 1. \tag{S49}$$

The solution can be obtained by using the exponential fundamental solution. This gives the explicit expression

$$\overline{C}_s^*(x, \lambda) = \exp\left[-\frac{x\overline{v}}{2D^*} \left(\sqrt{1 + 4\frac{(\lambda + \theta_h d^{-1}[\lambda\varphi_h^*(\lambda) + k_b\varphi_b^*(\lambda)])D^*}{\overline{v}^2}} - 1 \right) \right]. \tag{S50}$$

B. Stream concentration in surrogate model *S1*

We consider the scenario that the entire hyporheic zone is characterized by a constant reactivity, which is used in the main text to define a constant equivalent reactivity for the streambed.

We set $k(z) = k_e = $ constant. In this case, the transport equation (2) simplifies to

$$\partial_t \left[\overline{C}_e + \frac{\theta_h}{d} \int_0^t dt' \, \varphi_e(t - t')\overline{C}_s(t') \right] + \overline{v}\partial_x \overline{C}_e - \overline{D}^* \partial_x^2 \overline{C}_e = -\frac{\theta_h k_e}{d} \int_0^t dt' \, \varphi_e(t - t')\overline{C}_e(t'), \tag{S51}$$

where $\overline{C}_e$ is the vertically averaged water column concentration, and the reactive memory function is given by

$$\varphi_e(t) = \phi(t) \exp(-k_e t), \tag{S52}$$

and in Laplace space

$$\varphi_e^*(\lambda) = \phi^*(\lambda + k_e). \tag{S53}$$

The conservative memory function $\phi(t)$ is defined in Laplace space by

$$\phi^*(\lambda) = \sqrt{\frac{D_h}{\lambda}} \tanh(\sqrt{\lambda\tau_h}). \tag{S54}$$

The solution of (S51) for the boundary condition $\overline{C}_0^*(x = 0, t) = \delta(t)$ reads in Laplace space as

$$\overline{C}_e^*(x, \lambda) = \exp\left[-\frac{x\overline{v}}{2D^*} \left(\sqrt{1 + 4\frac{[\lambda + \theta_h d^{-1}(\lambda + k_e)\phi^*(\lambda + k_e)]D^*}{\overline{v}^2}} - 1 \right) \right]. \tag{S55}$$

SI-IV. EFFECTIVE REACTION RATE IN THE STREAMBED

The effective reaction rate k_e in *S1* is defined such that the reacted mass in response to a solute pulse is equal to the reacted mass in the MIM-B model. The reacted mass in the HZ in response to a point injection is obtained by integration of (S15) over the reactive region of the HZ. Thus, we obtain

$$M_R(t) = k_b \int_0^t dt' \, \varphi_B(t') \tag{S56}$$

for the MIM-B model and

$$M_R(t) = k_e \int_0^t dt' \, \varphi_e(t') \tag{S57}$$

We set the total reacted mass equal. This implies

$$k_e \int_0^\infty dt' \, \varphi_e(t') = k_b \int_0^\infty dt' \, \varphi_b(t') \tag{S58}$$

In Laplace space, the equation reads as

$$k_e \varphi_e^*(0) \equiv k_b \varphi_b^*(0). \tag{S59}$$

Using expressions (S30), (S32) and (S33), as well as (S53) and (S54) gives Equation (3) in the main text.

SI-V.   APPARENT RETARDATION COEFFICIENT AND REACTION RATE

Explicit expressions for the apparent retardation coefficient and reaction rate are obtained by expressing the integral terms in Eq. (5) in terms of the Laplace transformed memory functions. This gives

$$R_a = 1 + \frac{\theta_h}{d} \varphi_h^*(0), \qquad\qquad\qquad k_a = \frac{\theta_h k_b}{d} \varphi_b^*(0) \qquad (S60)$$

Using that $\varphi_h(t) = \varphi_b(t) + \varphi_0(t)$ and the explicit expressions (S30) for $\varphi_b^*(\lambda)$ and (S32) for $\varphi_0^*(\lambda)$, we obtain

$$R_a = 1 + \frac{\theta_h}{d} \left[\frac{\sqrt{D_h \tau_0}}{\cosh(\sqrt{k_b \tau_b})} + \sqrt{\frac{D_h}{k_b}} \tanh\left(\sqrt{k_b \tau_b}\right) \right] \qquad (S61)$$

$$k_a = \frac{\theta_h}{d} \sqrt{D_h k_b} \tanh\left(\sqrt{k_b \tau_b}\right). \qquad (S62)$$

SI-VI.   DIRECT NUMERICAL SIMULATIONS

The direct numerical simulations are based on the time-domain random walk method (TDRW) outlined in Russian *et al.* [4] for conservative solutes. In this framework, reactions in the biolayer are modeled by assigning a survival probability to each particle in the biolayer. For each TDRW step of duration τ, the survival probability is $\exp(-k_b \tau)$. A Bernoulli trial decides whether the particle survives or reacts at each step. To ensure that our results are consistent with continuum assumptions in our analytical model, we restrict our analysis to times greater than the characteristic residence time in a single grid cell. For all simulations, $D_h = 1.042 \times 10^{-6} \, \mathrm{m^2 \, s^{-1}}$ and $h = -2 \, \mathrm{m}$, and $\theta_h = 1$. Porosity of the subsurface only rescales d and therefore is set to 1 without loss of generality (S48).

Memory function (i.e., streambed-scale) simulations are designed to mimic a pulse injection at the SWI. We release N_0 particles in the first grid cell below the SWI, and we quantify the total number of particles remaining in the HZ. For all simulations $b = -0.05 \, \mathrm{m}$, and the grid resolution is set to $\Delta z = 5 \times 10^{-2} \, \mathrm{m}$. Parameter k_b is varied to achieve a range of Da.

Reach-scale simulations are designed to mimic a pulse tracer injection commonly performed in field experiments. We release N_0 particles uniformly in the mobile zone at $x = 0 \, \mathrm{m}$ and $t = 0 \, \mathrm{s}$. Breakthrough curves (BTCs) are given by the distribution of particle arrival times at a downstream distance x. We vary $0.02 \leq |b| \leq 0.5 \, \mathrm{m}$ across simulations while holding other parameters constant. For all experiments, $d = 0.05 \, \mathrm{m}$, $v_0 = 0.005 \, \mathrm{m \, s^{-1}}$, $\overline{v} = 0.05 \, \mathrm{m \, s^{-1}}$, $D^* = 0.0015 \, \mathrm{m^2 s^{-1}}$, and $k_b = 2.0 \times 10^{-4} \, \mathrm{s^{-1}}$. The grid resolution is set to $\Delta z = 2 \times 10^{-2} \, \mathrm{m}$.

SI-VII.   FIELD COMPARISON

We compared simulated and modeled Da to values of Da estimated from Schaper *et al.* [5], to understand the expected range of Da for trace contaminants in natural streams. We limited the comparison to results that met the following criteria:

- profiles of first-order solute reactions were reported as a function of depth in the hyporheic zone,

- no production of mass was inferred (i.e., all values of $k(z)$ were greater than zero),

- $k(z)$ decreased to a nominal value by the deepest measurement location, indicating the presence of a benthic biolayer and an inert sublayer.

For each solute, we determined whether the reported $k(z)$ was best approximated by a slab (i.e., constant rate) or by an exponential profile. Profiles that showed a sharp transition to values near $k(z) = 0$ were considered to be a slab with $z = -b$ equal to the transition depth, and k_b equal to the arithmetic average of $k(z)$ for all depths above $z = -b$. For profiles that showed a gradual decrease to near-zero values by the lowest measurement location, we determined k_b and b by fitting an exponential profile to $k(z)$. If dispersion coefficients and retardation coefficients R were reported as a function of depth, we approximated D_h as a constant value equal to the harmonic mean of $D_h(z)$ measured at all depths above $z = -b$ [6]. Similarly, we approximated a constant R as the arithmetic average of all R above $z = -b$. For consistency with our model assumptions, advective velocities reported in the biolayer were set to zero, meaning

Da estimates are biased slightly higher than in conditions reported since downwelling conditions in this study suggest a shorter residence time in the biolayer. We calculated Da as

$$Da = \frac{k_b b^2}{R D_h}$$

All values are reported in Table I. These values span a wide range of effective streambed reactivities, as shown in Figure S1.

Table I: Literature values of Da

| Chemical	Source	D_h ($\times 10^{-6}$ m^2 s^{-1})	R	profile shape	k_b ($\times 10^{-4}$ s^{-1})	b ($\times 10^{-2}$ m)	Da
metoprolol	Schaper et al., 2019	1.0	4.5	exp	16.1	8.6	$5.5\times10^{+01}$
gabapentin	Schaper et al., 2019	1.0	1.4	exp	6.8	11.6	$1.3\times10^{+01}$
gabapentin-lactam	Schaper et al., 2019	1.0	1.3	slab	0.8	5.0	2.8×10^{-01}
valsartan	Schaper et al., 2019	1.0	1.9	slab	1.7	5.0	8.1×10^{-01}
sotalol	Schaper et al., 2019	1.0	1.9	exp	3.7	10.5	$8.0\times10^{+00}$
metformin	Schaper et al., 2019	1.0	15.3	exp	1.9	38.5	$4.3\times10^{+02}$
guanylurea	Schaper et al., 2019	1.0	2.6	exp	4.0	18.5	$3.6\times10^{+01}$
benzotriazole	Schaper et al., 2019	1.0	4.0	exp	2.8	14.5	$2.4\times10^{+01}$
4-formylaminoantipyrine	Schaper et al., 2019	1.0	2.4	slab	1.5	5.0	9.3×10^{-01}
methylbenzotriazole	Schaper et al., 2019	1.0	3.3	exp	1.5	17.0	$1.5\times10^{+01}$
candesartan	Schaper et al., 2019	1.0	1.7	slab	1.7	5.0	7.2×10^{-01}
olmesartan	Schaper et al., 2019	1.0	1.4	slab	1.3	5.0	4.6×10^{-01}
tramadol	Schaper et al., 2019	1.0	2.2	slab	0.5	5.0	3.0×10^{-01}
carbamazepine	Schaper et al., 2019	1.0	3.6	slab	0.2	5.0	1.8×10^{-01}
dihydroxy-carbamazepine	Schaper et al., 2019	1.0	2.2	exp	0.9	10.5	$2.3\times10^{+00}$
diatrizoic acid	Schaper et al., 2019	1.0	1.1	slab	0.3	5.0	8.6×10^{-02}
dissolved organic carbon	Schaper et al., 2019	1.0	1.0	exp	1.1	16.4	$3.1\times10^{+00}$
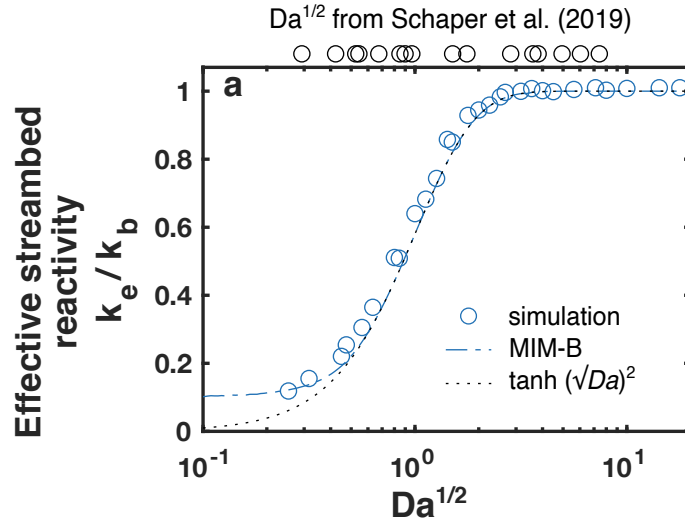
Figure S1: Measured and modeled reactivity across simulations and scales. Results closely match the approximation $k_e/k_b = \tanh\left(\sqrt{Da}\right)^2$, as described in the main text.

[1] H. B. Fischer, J. E. List, C. R. Koh, J. Imberger, and N. H. Brooks, *Mixing in inland and coastal waters* (Academic press, 1979).

[2] H. Carslaw and J. Jaeger, Oxford: Clarendon Press (1959).

[3] M. Abramowitz and I. A. Stegun, *Handbook of mathematical functions with formulas, graphs, and mathematical tables*, Vol. 55 (US Government printing office, 1964).

[4] A. Russian, M. Dentz, and P. Gouze, Water Resources Research **52**, 3309 (2016), publisher: Wiley Online Library.

[5] J. L. Schaper, M. Posselt, C. Bouchez, A. Jaeger, G. Nuetzmann, A. Putschew, G. Singer, and J. Lewandowski, Environmental Science & Technology **53**, 4224 (2019).

[6] M. Dentz, P. Gouze, A. Russian, J. Dweik, and F. Delay, Advances in Water Resources **49**, 13 (2012).